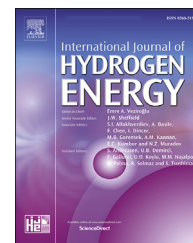


Available online at www.sciencedirect.com

ScienceDirect

journal homepage: www.elsevier.com/locate/he

Carbon-negative valorization of biomass waste into affordable green hydrogen and battery anodes

Hanmin Yang^a, Anissa Nurdiawati^b, Ritambhara Gond^c, Shiwei Chen^d, Shule Wang^{e,f}, Bin Tang^g, Yanghao Jin^a, Ilman Nuran Zaini^a, Ziyi Shi^a, Wujun Wang^h, Andrew Martin^h, Reza Younesi^c, Linda Sandströmⁱ, Pär G. Jönsson^a, Weihong Yang^a, Tong Han^{a,*}

^a Department of Materials Science and Engineering, KTH Royal Institute of Technology, SE-10044 Stockholm, Sweden

^b Department of Industrial Economics and Management, KTH Royal Institute of Technology, 10044 Stockholm, Sweden

^c Department of Chemistry - Ångström Laboratory, Structural Chemistry, Uppsala University, Lägerhyddsvägen 1, 751 21 Uppsala, Sweden

^d University of Michigan-Shanghai Jiao Tong University Joint Institute, Shanghai Jiao Tong University, 800 Dong Chuan Rd., Minhang District, Shanghai, 200240, PR China

^e International Innovation Center for Forest Chemicals and Materials, College of Chemical Engineering, Nanjing Forestry University, Longpan Road 159, Nanjing, 210037, China

^f Jiangsu Province Key Laboratory of Biomass Energy and Materials, Institute of Chemical Industry of Forest Products, Chinese Academy of Forestry (CAF), No. 16, Suojin Five Village, Nanjing, 210042, China

^g Engineering Research Center of Advanced Functional Material Manufacturing of Ministry of Education, School of Chemical Engineering, Zhengzhou University, Zhengzhou, 450001, PR China

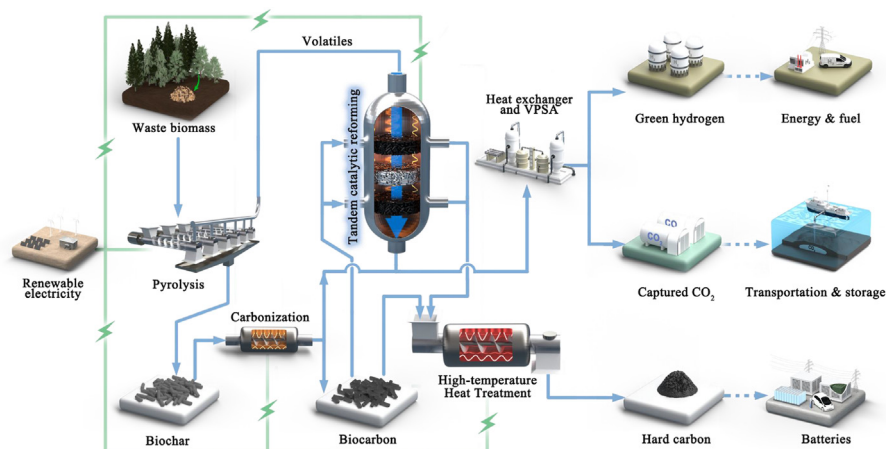
^h Department of Energy Technology, KTH Royal Institute of Technology, Brinellvägen 68, 100 44 Stockholm, Sweden

ⁱ RISE AB, Division Bioeconomy and Health, Biorefinery and Economy, Box 726, SE-941 28, Piteå, Sweden

HIGHLIGHTS

- Fully valorization of biomass into hydrogen, battery anodes, and negative emission.
- Tandem biocarbon + NiAlO + biocarbon catalyst reform pyro-vapors into H₂-rich syngas.
- High-performance SIB anodes with 263 Wh/kg of capacity and 89% of ICE.
- A sustainable and profitable bio-refinery realizing payback period within two years.

GRAPHICAL ABSTRACT



* Corresponding author.

E-mail address: tongh@kth.se (T. Han).

<https://doi.org/10.1016/j.ijhydene.2023.09.096>

0360-3199/© 2023 The Author(s). Published by Elsevier Ltd on behalf of Hydrogen Energy Publications LLC. This is an open access article under the CC BY license (<http://creativecommons.org/licenses/by/4.0/>).

ARTICLE INFO

Article history:

Received 10 July 2023

Received in revised form

31 August 2023

Accepted 9 September 2023

Available online 26 September 2023

Keywords:

Affordable energy

Biorefinery

Hydrogen

Negative emission

Battery anode

ABSTRACT

The global Sustainable Development Goals highlight the necessity for affordable and clean energy, designated as SDG7. A sustainable and feasible biorefinery concept is proposed for the carbon-negative utilization of biomass waste for affordable H₂ and battery anode material production. Specifically, an innovative tandem biocarbon + NiAlO + biocarbon catalyst strategy is constructed to realize a complete reforming of biomass pyro-vapors into H₂+CO (as a mixture). The solid residues from pyrolysis are upgraded into high-quality hard carbon (HCs), demonstrating potential as sodium ion battery (SIBs) anodes. The product, HC-1600-6h, exhibited great electrochemical performance when employed as (SIBs) anodes (full cell: 263 Wh/kg with ICE of 89%). Ultimately, a comprehensive process is designed, simulated, and evaluated. The process yields 75 kg H₂, 169 kg HCs, and 891 kg captured CO₂ per ton of biomass achieving approx. 100% carbon and hydrogen utilization efficiencies. A life cycle assessment estimates a biomass valorization process with negative-emissions (−0.81 kg CO₂/kg-biomass, reliant on Sweden wind electricity). A techno-economic assessment forecasts a notably profitable process capable of co-producing affordable H₂ and hard carbon battery anodes. The payback period of the process is projected to fall within two years, assuming reference prices of 13.7 €/kg for HCs and 5 €/kg for H₂. The process contributes to a novel business paradigm for sustainable and commercially viable biorefinery process, achieving carbon-negative valorization of biomass waste into affordable energy and materials.

© 2023 The Author(s). Published by Elsevier Ltd on behalf of Hydrogen Energy Publications LLC. This is an open access article under the CC BY license (<http://creativecommons.org/licenses/by/4.0/>).

1. Introduction

Energy security and environmental pollution have become major global concerns [1]. The present energy system faces challenges related to global warming and fossil fuels depletion, demanding immediate action through the use of renewable energy sources. Affordable and clean energy production from biomass waste has the potential to decouple energy production from fossil resources and the resulting CO₂ emissions. This could significantly aid in attaining the global sustainable development goals and the 2030 Agenda for Sustainable Development [2,3]. Moreover, achieving negative emissions from renewable and carbon-neutral resources is considered essential [4,5] to fulfill the goals of the Paris Agreement. Therefore, it is a clear priority for future biomass research to explore the utilization of biomass waste for producing affordable and clean energy with negative emissions [6].

The implementation of biorefinery processes based on renewable bio-resources, mainly lignocellulosic biomass, has become of paramount importance in light of the impending future energy demand [7–9]. The main challenge associated with lignocellulosic biorefinery approaches lies in the realm of conversion technologies [10]. Currently, the existing lignocellulosic biorefineries based on thermochemical routes mainly involve the separate valorization of lignin, cellulose, hemicellulose into value-added products. Due to the distinct structures and different physicochemical properties of lignin, cellulose, and hemicellulose, a uniform strategy cannot be applied to generate valuable products from all these components. As a result, an integrated biorefinery approach and process optimization are imperative. Liao et al. [11] developed an integrated biorefinery with a low-carbon footprint. Their proposed integrated biorefinery achieved conversions of 78

and 76 wt%, respectively, of the initial mass and carbon content of birch wood being economically and sustainably valorized into four high-value end-products.

Nonetheless, integrated biorefinery approaches necessitate meticulous design to uplift the product valorization rates and economic value along with the optimization of mass and energy flow through the system. The technologies should be uncomplicated, resilient, and concurrently economically viable and eco-friendly. It is obvious that the existing process required further improvements in terms of economics, technological improvements and appropriate process integrations to reduce the environmental burdens.

The cost-effective production of H₂ and carbon-based battery anodes from biomass waste, coupled with the capture of CO₂, is believed to be one of the ideal biorefineries for the future [12]. H₂ stands as one of the most promising clean energy carriers in the future [2,13]. Augmenting the production of renewable H₂ from biomass could significantly contribute to global decarbonization efforts [14]. The production of high-quality battery-grade carbon from abundant and renewable biomass resources serves to address the substantial demands for batteries driven by the continuously expanding markets of portable electronics and electric vehicles [15,16]. Captured CO₂ can be sequestered within subterranean geological formations, manifesting as negative emissions. Envisioning a sustainable and lucrative biorefinery that achieves negative emissions holds significant promise and represents a pioneering effort [17]. Projects involving transport and storage of industry-captured CO₂ have been initiated in Europe [18], facilitating the integration of negative emissions with biorefinery systems.

In this work, a novel biorefinery is developed to produce affordable H₂ and battery carbon anodes, concurrently

achieving negative emissions (Fig. 1). A biomass pyrolysis and in-line catalytic reforming process was developed to convert pyro-vapors into syngas characterized by elevated $H_2 + CO$ concentrations. A remarkably effective and stable biocarbon + NiAlO + biocarbon reforming catalyst was innovated and examined for the first time. Its primary function is to enable complete conversion of the volatiles derived from pyrolysis into syngas ($H_2 + CO$) and water, serving as the foundational aspect of this study. Meanwhile, a two-step thermal treatment process of biochar was integrated to convert it into high-quality hard carbons (HCs), which are employed as anodes in sodium-ion batteries (SIBs). The electrochemical performance of HCs was assessed in both half-cell and full-cell batteries. The effect of the thermal treatment conditions on the structure of HCs and the correlation between their structure and electrochemical performance were elucidated. Based on the experimental results, a sustainable biorefinery business paradigm is simulated and assessed, with H_2 , battery carbon and captured CO_2 being envisioned as final products.

Compared to the existing biorefineries, our proposed biorefinery process accomplished comprehensive utilization of biomass waste through relatively straightforward and resilient technologies, thereby attaining elevated resource efficiency and negative carbon emissions. Consequently, this approach serves to furnish established and emerging markets with high-value-added end products.

2. Materials and methodology

2.1. Materials

2.1.1. Biomass

The used biomass in this study was a pine and spruce mixture obtained from Svenska Cellulosa AB (SCA). The properties of the biomass feedstock are listed in Table S1. Prior to conducting the experiments, the biomass samples were subjected to drying in an oven at $105\text{ }^\circ\text{C}$ until a consistent weight was

achieved. Subsequently, the samples underwent sieving, and particles within the size range of 1–1.25 mm were selected for further use.

2.1.2. Catalyst

The biocarbon catalyst used for carbon reforming in this work was prepared via the thermal treatment of biomass pyrolysis biochar (denoted as biocarbon-500) at a temperature of $800\text{ }^\circ\text{C}$ for 3 h in this work, denoted as biocarbon-800. Thereafter, biocarbon in a particle size range of 1–1.25 mm was used in order to reach a reasonable pressure drop. The element composition of biochar and biocarbon can also be seen in Table S1.

$NiAl_2O_4$ spinel-type catalyst (NiAlO spinel) was prepared via impregnating $Y-Al_2O_3$ support with an aqueous solution of nickel (II) nitrate hexahydrate ($Ni(NO_3)_2 \cdot 6H_2O$). $Ni(NO_3)_2 \cdot 6H_2O$ (99.9985%) and $Y-Al_2O_3$ (1/8 in. pellets) were both purchased from Alfa Aesar company. In this study, the loading of Ni in the catalyst was 10 wt %. To prepare the catalyst, $Y-Al_2O_3$ pellets were initially ground into powder form. Subsequently, the powdered $Y-Al_2O_3$ was impregnated with $Ni(NO_3)_2 \cdot 6H_2O$ solutions. The mixture was then placed at room temperature under magnetic stirring for 3 h to achieve complete impregnation. Thereafter, the slurry was put in a drying oven at $105\text{ }^\circ\text{C}$ overnight. Finally, the catalyst was calcined in a muffle furnace at $750\text{ }^\circ\text{C}$ for 3 h. Afterward, the catalyst was subjected to calcination in a muffle furnace at a temperature of $750\text{ }^\circ\text{C}$ for a duration of 3 h. Prior to conducting the experiments, the prepared catalyst underwent grinding and sieving to achieve a particle size range of 1–1.25 mm.

2.2. Biomass pyrolysis and in-line catalytic reforming over tandem biocarbon + NiAlO spinel + biocarbon catalyst

In this study, biomass pyrolysis and in-line catalytic reforming over tandem biocarbon + NiAlO spinel + biocarbon catalyst tests were all conducted using a two-stage reactor, which is depicted in Fig. S1. The entire system comprises several

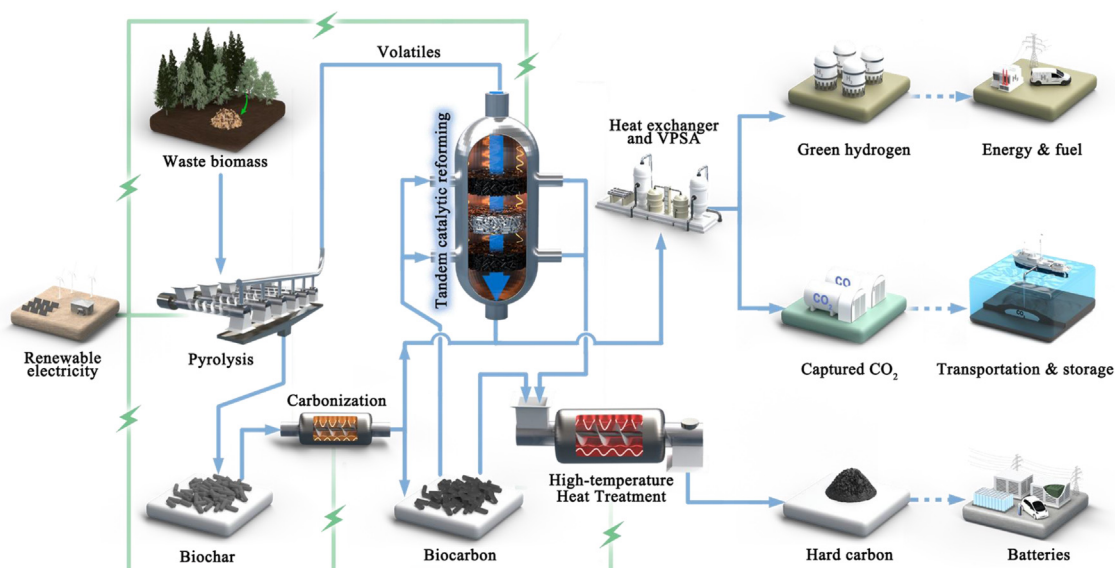


Fig. 1 – Carbon-negative valorization of biomass waste into affordable green hydrogen and battery anodes. (For interpretation of the references to color in this figure legend, the reader is referred to the Web version of this article.)

sections, including a carrier gas supply section, a two-stage fixed-bed reactor, a cooling section, and an online gas collection and analysis section. The two-stage reactor system consists of two furnaces, with the left furnace serving as the pyrolysis reactor and the right furnace as the catalytic reforming reactor. Prior to the experiments, the catalytic reforming reactor was loaded with a layered arrangement of 5 g of biocarbon, 5 g of Ni–Al spinel catalyst, and another 5 g of biocarbon. Additionally, 10 g of biomass sample was pre-stored in a short storage tube. Nitrogen (N₂) gas was used as carrier and protective gas, which was introduced into the system at a flow rate of 200 mL/min. The pyrolysis reactor and the catalytic reforming reactor were then heated to their respective set temperatures: 500 °C for pyrolysis and 800 °C for catalytic reforming. Once both reactors reached the desired temperatures, the biomass sample was fed into the pyrolysis reactor to initiate the test. The resulting upgraded volatiles were subsequently condensed by passing through a series of cooling bottles immersed in a cooling bath maintained at –15 °C. Non-condensable gas was collected in a 25 L Tedlar™ gas bag for further analysis.

2.3. Two-step thermal treatment of biochar

Biochar produced from the biomass pyrolysis process was further upgraded by a two-step thermal treatment. The carbonization process was conducted at a temperature of 800 °C in an inert atmosphere using N₂ gas. The main aim of this process was to remove all volatiles, resulting in biocarbons as catalysts and hard carbon precursors. Biochar collected from the pyrolysis reactor was moved to a silica boat and put into the reactor. Then nitrogen with a 200 mL/min flowrate was also introduced as carrier gas. The reactor was heated up to 800 °C with a heating rate of 30 °C. After reaching the temperature, the temperature was kept for 3 h.

Then a high-temperature heat-treatment of biocarbon including spent biocarbon catalysts was conducted in order to produce HCs which can be used as SIBs anodes. An induction furnace was used for the high-temperature heat-treatment. Biocarbon powders were put into a graphite crucible and then move to the induction furnace. A refractory brick cover made of aluminum oxide was wrapped around the graphite crucible to reduce the heat loss during the heat treatment. Argon with a flow rate of 500 mL/min was used as carrier and protective gas to ensure an inert atmosphere and the graphite crucible was heated up evenly to the set temperature. Two different heating temperatures i.e. 1400 °C and 1600 °C and two different heat treatment duration time i.e. 3 h and 6 h were tested with aiming to study the correlation between the electrochemical performance and the structure of HCs.

2.4. Sodium battery assembly and anode performance test

2.4.1. Half cell test

To prepare the carbon electrode for electrochemical measurements, the hard carbon, super P carbon black (Imerys Graphite & Carbon, France), and sodium alginate (Shanghai Aladdin Biochemical Technology Co., Ltd, China) binder were mixed in deionized water solvent with a weight ratio of 9:0.5:0.5 to make

a slurry, which was then cast on a copper foil by the doctor blade method. The electrode was dried at 120 °C under vacuum for 12 h and afterward was cut into 12 mm diameter circular pieces for coin cell assembly. The mass loading of the active material was controlled between 1.5 and 2 mg cm⁻¹. The liquid electrolyte was 1 M NaPF₆ in ethylene carbonate (EC) and dimethyl carbonate (DMC) (1:1 in volume), and pure sodium foil and glass fiber were utilized as the counter electrode and the separator, respectively. All the half-cells were assembled in CR2032 coin-type cells under an argon atmosphere in a glove-box. The discharge and charge tests were performed with a NETWARE CT-4000 battery test system in a voltage range of 0–2 V at a specific current of 20 mA/g under room temperature.

2.4.2. Full cell test

Commercial Prussian white (PW) electrodes of 94 wt% of active material were provided by Altris AB, which had a capacity loading of approximately 1.12 mAh/cm². The full cell was made using hard carbon electrodes of the aforementioned type with a higher mass loading of 7.5 mg/cm². For electrochemical characterizations hard carbon against PW, 8 × 8 cm pouch cell was built under Ar- glove box using 1 M NaBF₄ in 1:1 mixture of G4: G2 (tetraethylene glycol dimethyl ether, G4: dimethyl ether G1, from Sigma Aldrich) electrolyte and 2 solupor separators. The charge and discharge tests were evaluated with a Land potentiostats battery test system in the voltage range of 3.9 V–1.3 V at a C/5 rate (20 mA/h) at room temperature.

2.5. Process modeling

Mass and energy balance models were produced using own experimental results and the best available data from the literature. The simulation results were used to analyze the system's technical feasibility based on energy efficiency. The analysis involves the simulation of two primary case scenarios. Case A is the co-production of hydrogen and HC from biomass with CO₂ capture. Case B represents a standalone syngas plant that co-produces syngas and HC.

The process modelling and calculation was conducted using the Aspen Plus version 11 (Aspen Technology, Inc.). Main process design parameters and assumptions used in the modelling are shown in Table S3.

- The processes are considered in steady-state conditions.
- Heat and pressure losses are assumed to be negligible.
- The inlet temperature of cooling water is 25 °C, and the return temperature is 45 °C.
- The ambient temperature and pressure are 25 °C and 0.1 MPa.
- The VPSA unit are modelled as black-boxes with the key energy consumptions estimated from the literature.

2.6. Life cycle assessment

Life cycle assessment (LCA) was conducted for the proposed wood biorefinery that produces three representative products—H₂, CO and HC—using two functional units: (1) 1 kg of processed biomass (2) 1 kg of product, either H₂, CO or HC.

The climate change impact category is in focus, where carbon footprint were estimated using a cradle-to-gate LCA approach. Cut-off allocation approach was adopted, so in our case, sawdust was assumed as waste material with no burden.

2.7. Economic evaluation

The economics of the proposed plant was assessed by calculating the break-even point (BEP), the payback period (PBP) and internal rate of return (IRR) assuming certain market prices. A minimum product selling price is determined to recover the initial investment plus a 10% rate of return considering 100% equity financing. It is calculated as the selling price of hydrogen (Case A) or syngas (Case B), which makes the net present value (NPV) of the project zero. PBP represents the time required for the cash flow to equal the original fixed-capital investment. The Internal Rate of Return (IRR) is the discount rate that makes the net present value (NPV) of a project zero. The economic parameters for the discounted cash flow analysis and the calculation of fixed capital cost and operating costs are described in Table S5.

3. Results and discussion

3.1. Development of a tandem biocarbon + NiAlO spinel + biocarbon reforming catalyst

3.1.1. Catalyst performance

Thermal reforming is currently the main means of producing syngas and H₂ from natural gas, hydrocarbons, coals, and biomass [19,20]. A biomass pyrolysis and in-line catalytic reforming process are conducted to convert biomass pyro-vapors into syngas. The key to our work is the construction of a highly efficient and stable tandem biocarbon + NiAlO spinel + biocarbon reforming catalyst (Fig. 1), which realized an entire reforming of pyro-vapors consisting of hundreds of substances [21] into water and syngas. A single testing cycle displayed a syngas yield as high as 745 mg/g-biomass, and the volumetric percentage of H₂+CO in the syngas was higher than 91% (Fig. 2A and B). After 15 testing cycles, the average yield of syngas was higher than 680 mg/g-biomass (Fig. 2C), and the volumetric percentage of H₂+CO in the syngas was maintained at a value higher than 83 vol% (Fig. 2D). The yields of H₂ and CO were higher than 21.00 mol/g-biomass and 17.00 mol/g-biomass, respectively, which contributed to a GECE value higher than 71% (Fig. 2D). More importantly, the main component of the resulting liquid is only water after all testing cycles, which indicates the tar issue could be greatly weakened by the deployment of the biocarbon + NiAlO spinel + biocarbon reforming catalyst [22].

3.1.2. How the Tandem Catalyst Operates

The reforming of pyro-vapors involves complex reaction networks, including hydrolysis, cracking, steam reforming, water gas shift, carbon gasification, etc. (Table S9) [23]. As illustrated by the scanning electron microscope (SEM) images, the fresh biocarbon catalysts (biocarbon-800) have regular macropores ranging between 20 and 30 μm (Fig. 3A-1 and 3A-2) with well-defined elongated channels in the axial direction

(Fig. 3A-1 and 3A-3). Based on the results of adsorption and desorption tests with N₂ and CO₂ gases, it's been observed that secondary micropores (ranging from 3.5 to 5.5 Å with CO₂ and ranging from 15 to 35 Å with N₂) exist on the channel walls (Fig. 3B, Fig. S6) [19]. The catalyst bed formed by a random accumulation of uniform-size biocarbon particles (1–1.25 mm) with a hierarchical pore structure could serve as a carbon filter to capture the fine biochar particles and soots formed in the process and decrease the tar issue (Fig. 3C). More importantly, the top biocarbon catalyst layer can also increase the tortuosity for gas molecules (Fig. 3C), while ensuring a relatively low-pressure drop (62 kPa/m, Table S2). As a result, the thermal cracking of heavy-molecular compounds was significantly promoted, increasing the proportion of hydrogen and light molecules (light hydrocarbons and light oxygenate) [24]. Notably, it could reduce the risk of the NiAlO spinel catalyst deactivation caused by coke deposition. The catalytic reforming of light molecules over steam/CO₂ (coexisting in the gas flow) to H₂ and CO was significantly promoted in the NiAlO spinel catalyst layer. The reducing gases in the vapors promote the gradual reduction of nickel in the spinel structure to form Ni⁰ (Fig. 3D), which is essential for the reforming performance of the NiAlO spinel catalyst [25,26]. Gradual reduction of the NiAlO spinel into Ni during the cycling test can be confirmed by comparing the XRD patterns of the spent NiAlO-single and the spent NiAlO-cycles (Fig. 3D). The residual condensable compounds in the pyro-vapors can be further cracked in the bottom biocarbon catalyst layer. Moreover, the biocarbon materials (both top and bottom layers) were also reacted with steam and CO₂ (by carbon gasification and Boudouard reaction) [27,28]. To summarize, the use of the tandem biocarbon + NiAlO spinel + biocarbon reforming catalyst enables the complex reactions to be selectively promoted on different catalyst layers, resulting in excellent catalytic performance as well as good stability (Fig. 3C).

3.1.3. Catalyst deactivation and regeneration

When looking at SEM images of fresh and spent biocarbon catalysts (Fig. 3A and Fig. S7, respectively), it becomes apparent that the top layer of the biocarbon catalyst was visibly shattered. This is evidenced by a decrease in particle size from a range of 1000–1200 μm (fresh biocarbon catalyst) to a range of 1–100 μm (spent biocarbon catalyst). This suggests that undergoing the reaction with volatiles rich in steam and carbon dioxide, the biocarbon catalyst is significantly shattered. Moreover, the coke produced by the promoted thermal cracking reactions remains in the biocarbon layer, attaching to the biocarbon particle surface (Fig. S7). The decreased specific surface area and total pore value of the spent biocarbon-upper catalyst compared to the fresh biocarbon catalyst indicated that the formed coke blocked the micro-pores (Table S10). The roughly equal weights of fresh and spent biocarbon catalysts (upper layer) indicated that the weight increase caused by coke formation compensates for the weight decrease caused by carbon gasification after 15 testing cycles (Table S11). It appears that as the reaction cycle increases, the biochar catalyst particles experience significant damage and coke attachment, resulting in severe blockages within their internal channels. As previously stated, the top layer of biocarbon contains elongated

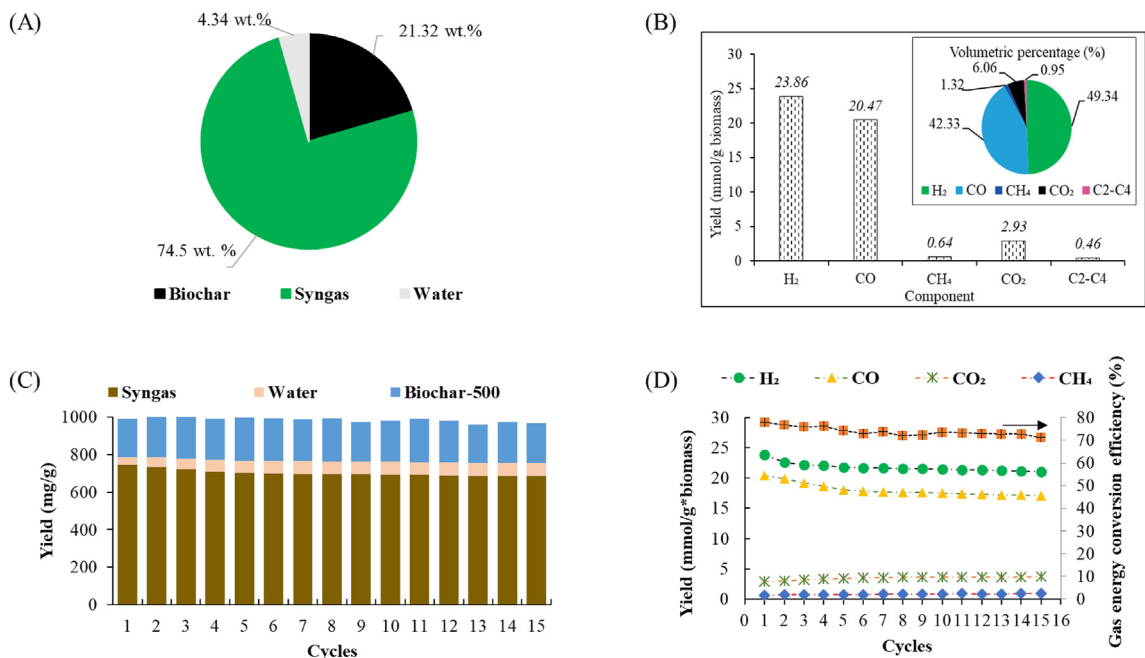


Fig. 2 – Tandem catalyst performance. A. Yields of syngas, water, and biochar-500 of a single test; B. Specific yields and volumetric percentage of gas components of a single test; C. Yields of syngas, water, and biochar-500 of different testing cycles; D. Specific yields of gas components and corresponding GECE of different testing cycles.

channels that effectively protect the NiAlO catalyst by pre-processing volatile compounds. This results in outstanding catalytic performance and stability. The loss of the channels of the biocarbon catalyst would be one of the major reasons for the gradual decrease in the catalytic performance during the cycling test. Fortunately, biocarbon catalysts are produced

from the identical biomass pyrolysis process. To address this issue in upscaling tests, it only needs to consider increasing the replacement frequency of the upper biochar catalyst.

The NiAlO spinel catalyst increased by 43% in weight after 15 cycles, indicating coke deposition on the catalyst (Table S11). This could also be the potential reason for the

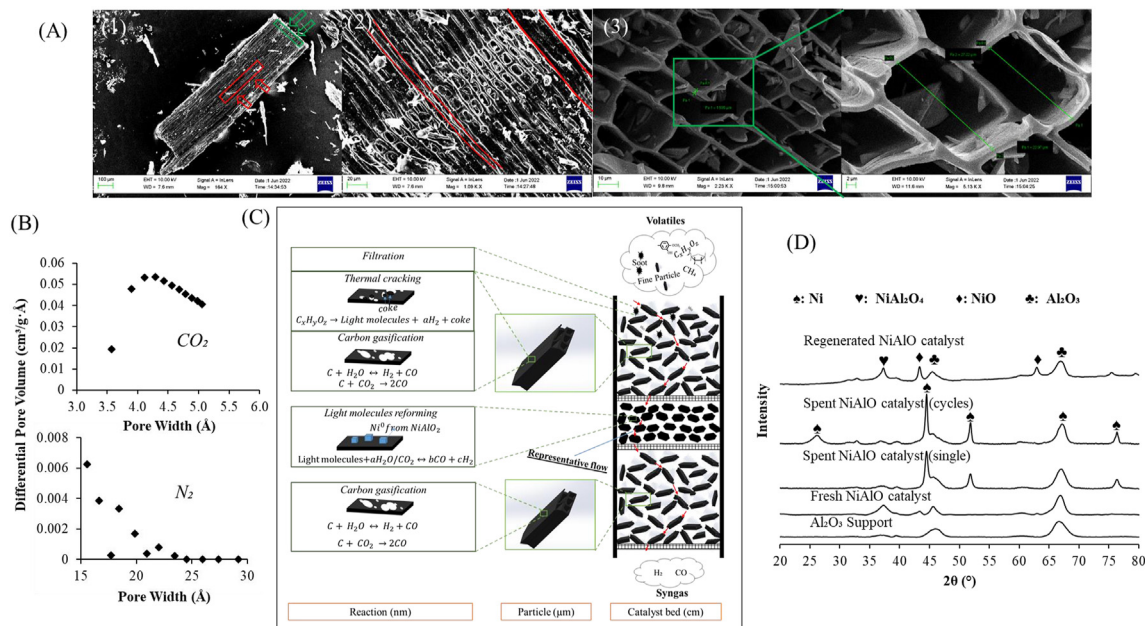


Fig. 3 – How the Tandem Catalyst Operates. A. Surface morphology of biocarbon catalyst; B. Pore size distribution of the biocarbon catalyst; C. Proposed catalytic mechanism of the tandem catalyst; D. XRD patterns of NiAlO spinel catalyst and Al₂O₃ support.

gradual decrease in the catalytic performance during the cycling test. According to two temperature-programmed oxidation characterization analyses, the coke deposited on the catalyst has distinct sources. It includes biochar from fragmented biocarbon particles and inert coke from catalytic reactions (Fig. 4B,C,D). The presence of biocarbon in the spent catalyst has also been confirmed through TPO analysis and SEM images of the catalyst. (Fig. 3E-2 and Fig. S8,S9). Therefore, an extra filter unit to capture broken biocarbon particles in upscaling test is suggested to be used. The catalyst is regenerated through incineration at 750 °C to eliminate all the deposited coke. The regenerated catalyst exhibits NiAlO spinel and NiO species, as observed in the XRD patterns displayed in Fig. 3D. This indicates that the spinel compound configuration can be partially restored. There appears to be little distinction between the fresh and spent catalyst when examining SEM images. However, a nickel loading reduction from 10 wt % to 8.4 wt % is detected by the inductively coupled plasma mass spectrometry (ICP-MS) analysis (Table S16). This indicates the irreversible loss of active metals due to the coke deposition, which is a common issue for nickel-based catalysts. In experiments conducted under identical conditions, a new tandem catalyst consisting of fresh biocarbon and regenerated NiAlO catalyst demonstrated comparable gas composition and yield to the cycling test (Table S14). This indicates that the catalyst's activity is not entirely deactivated.

To sum it up, the gradual deactivation of the tandem catalyst can be attributed to the loss of channels in the biocarbon catalyst in the upper layer and the formation of coke on the NiAlO. Determining which factor had a greater impact on the decrease in activity is a challenging task. The loss of active sites in the NiAlO catalyst is the major issue to

be resolved in the upscaling test. It is essential to have a suitable strategy for NiAlO catalyst regeneration and replacement.

3.2. HC production from biochar and its electrochemical performance as SIB anodes

3.2.1. Overall yield of the entire process

In addition to syngas and liquid, biomass pyrolysis could also yield approximately 213 mg/g-biomass of biochar (denoted as Biocarbon-500, Fig. 2A). A two-step thermal treatment process for biochar upgrading was performed to produce high-quality HCs as SIB anodes. Compared to the one-step carbonization process reported so far [29], the two-step carbonization process can maximize biochar's utilization efficiency while eliminating the limitations of industrial high-temperature carbonization furnaces. Therefore, it is more practical and more conducive to large-scale production. A carbonization process at a temperature of 800 °C for 3 h was performed to ensure a complete de-volatilization of biocarbon-500. This process further yielded 14.6 wt% of syngas, 3.9 wt% of water, and 81.5 wt% of biocarbon-800 based on the weight of biocarbon-500 (Fig. S10). The yields of H₂ and CO were 5.83 and 2.08 mmol/g-biocarbon-500, respectively (Table S12), leading to a 1.3 mmol/g-biomass increase in H₂ yield and 0.4 mmol/biomass increase in CO yield (Fig. 5A, Table S12). Overall, 169 mg of HCs, over 22 mmol of H₂, and 17 mmol of CO can be produced per gram of biomass waste of all testing cycles (Fig. 5B). The overall carbon and hydrogen conversion efficiencies of feedstock to valuable products (HCs, H₂, CO) were higher than 90% and 85%, respectively (Fig. 5B). Considering CO₂ also as an end-product, the carbon efficiency of feedstock

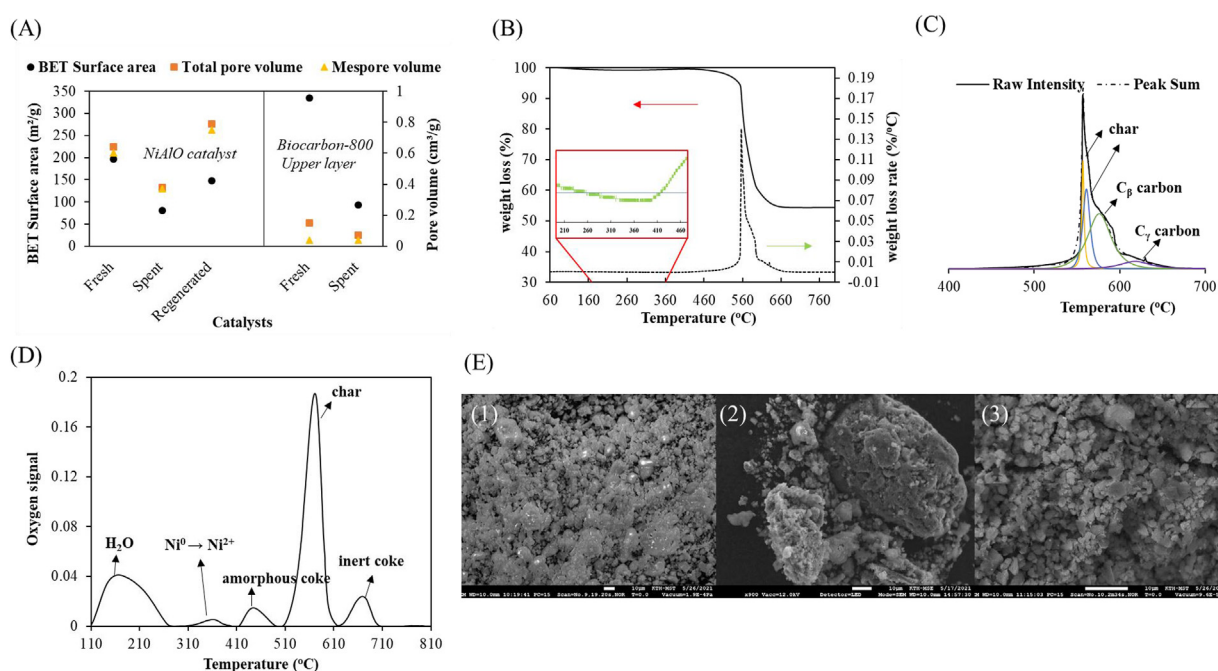


Fig. 4 – Catalyst deactivation and regeneration. A. Textural properties of fresh and spent biocarbon and NiAlO catalysts; B. TPO analysis of spent NiAlO spinel catalyst (15 cycles)-weight loss as temperature increased; C. Econvoluted derivative thermogravimetry (DTG) pattern of the TGA curve. D. TPO analysis of spent NiAlO spinel catalyst (15 cycles)- oxygen consumption as temperature increased. E. SEM images of fresh, spent and regenerated NiAlO catalyst.

can reach almost 100% and the hydrogen efficiency of feedstock is even higher than 100%.

3.2.2. Electrochemical performance

High-temperature heat treatment of biocarbon-800 at a temperature of 1600 °C for 3 and 6 h was conducted to produce high-quality HCs, denoted as HC-1600-3h and HC-1600-6h. The use of a processing temperature of 1600 °C is based on literature reports [30,31]. Notably, the spent biocarbon-800 catalysts could also apply to the high-temperature heat treatment to produce HCs. The replacement of the spent biocarbon catalysts was therefore not assumed to contribute to mass losses to the process. As illustrated in Fig. 5C, HC-1600-3h and HC-1600-6h show much higher I_G/I_D values than biocarbon-800, indicating a much more orderly structure. Moreover, a 2D peak corresponding to the graphene layers was detected for HC-1600-3h and HC-1600-6h, but not for biocarbon-800. Compared to HC-1600-3h, HC-1600-6h showed a higher I_G/I_D value indicating the increased formation of nano graphitic domains. HC-1600-3h and HC-1600-6h showed the same d-space values. This indicated that the increased duration did not significantly change the distance between graphene layers. Apart from forming nano graphitic domains, the closing of the open pores in the biocarbon-800 by the thermal treatment was another main reason. The pore size distribution results detected by CO₂ and N₂ (Fig. 3B) showed that the open pores in HC-1600-3h and HC-1600-6h, especially in the range between 15 and 25 Å, almost disappeared. And the volume of the pores detected by CO₂ in the range between 3 and 5 Å of HC-1600-3h and HC-1600-6h was also much smaller than that of the biocarbon (Table S13). Compared to HC-1600-3h, HC-1600-6h showed even lower pore volume and surface

area (Table S13), indicating a further closing of the pores. The TEM images of HC-1600-6h clearly showed the existence of nano graphitic domains and closed pores, as illustrated in Fig. 5D.

The target application of HCs is used as the anode material for sodium-ion batteries (SIBs). The electrochemical performance of HCs was evaluated first by half-cell test. At the current density of 20 mA/g, HC-1600-3h delivered a reversible capacity of 212 mAh/g with a high initial coulombic efficiency (ICE) of 84% (Fig. S11, Fig. 6A). HC-1600-6h delivered a higher reversible capacity of 252 mAh/g with a high ICE value of 83% (Fig. S12, Fig. 6B). The full-cell test is the final step for applying HCs into the market. Pouch-type full cells were assembled by using commercial Prussian White (PW; Na_xFe[Fe(CN)₆]; x > 1.9) as cathode and HC-1600-6h as an anode to evaluate the practical application prospect of HCs. The full cells delivered a high ICE value of 89% and a high reversible specific capacity of approximately 134 mAh/g based on the mass of the anode at 0.2 C (20 mA/h) for a voltage range from 1.3 to 3.9 V with an average operation voltage of 3.2 V (Fig. 6C). After 100 cycles, the full cells retained the specific capacity of approximately 111 mAh/g, corresponding to 83% capacity retention (Fig. 6D). The coulombic efficiency (except the ICE) values were retained higher than 99.6% (Fig. 6D). For the full cells (considering both the cathode and anode materials), a relatively high energy density of 263 Wh/kg was obtained. All of these values exhibited by the full cell are superior to the currently reported full-cell SIBs that use HC-based anodes (160 Wh/kg, CATL) [32,33]. These promising properties demonstrated that the HC-1600-6h derived from commercially available woody biomass waste is a promising anode for SIBs. The increased ICE values and the improved electrochemical performance

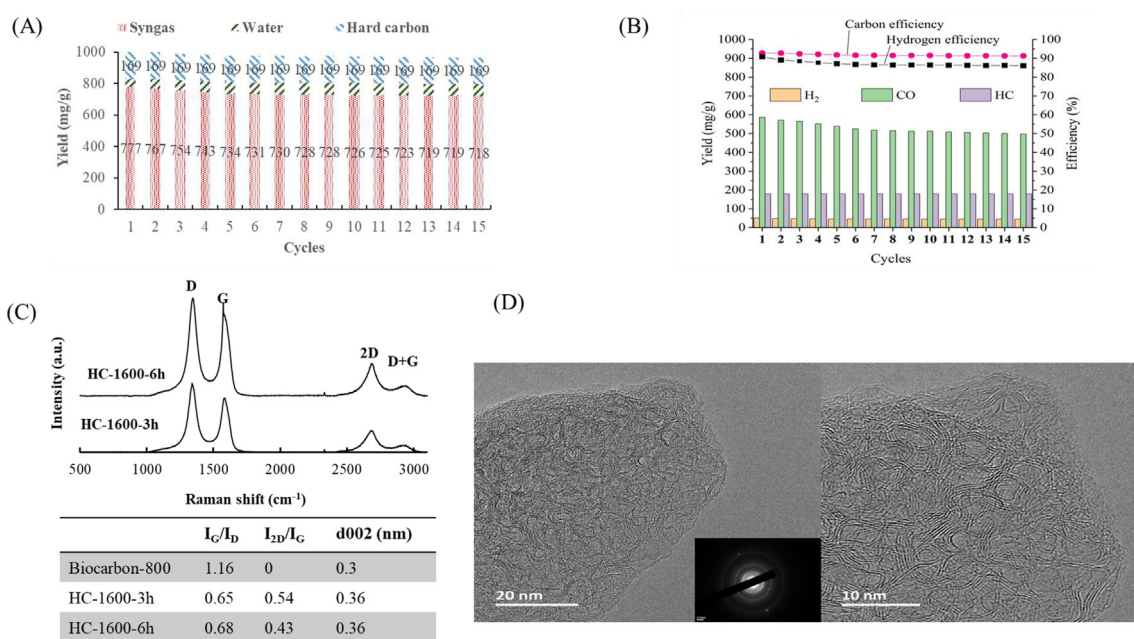


Fig. 5 – The overall yield of the entire process and the characterization of hard carbon samples. A. Mass balance results from the overall biorefinery process; B. Specific yields of main products i.e. H₂, CO, and HCs, and the carbon and hydrogen efficiency of the overall biorefinery process; C. Raman patterns of the hard carbon samples; D. TEM images of the hard carbon samples.

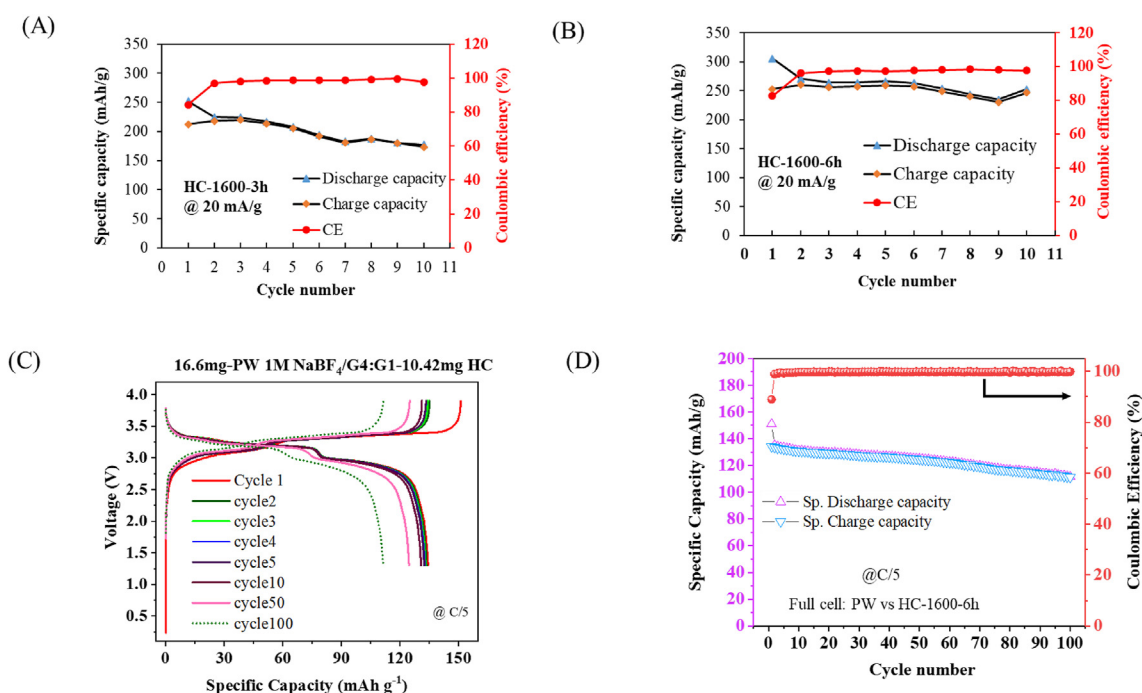


Fig. 6 – Electrochemical performance of the hard carbon samples. A. Cyclic capability of HC-1600-3h at a current density of 20 mA/g; B. Cyclic capability of HC-1600-6h at a current density of 20 mA/g; C. Cycling performance of the Prussian White/HC-1600-6h full-cell at a current rate of 0.2C-galvanostatic charge/discharge curves; D. Cycling performance of the Prussian White/HC-1600-6h full-cell at a current rate of 0.2C-cyclic capacity.

were attributed to the fact that the formation of nano graphitic domains from amorphous carbon is significantly promoted. Moreover, the HC-1600-6h structure rich in nano graphitic domains and closed pores demonstrated superior electrochemical performance [30,34]. In the full-cell test, using an ether-based electrolyte led to a further increase in the ICE (89%), which implied less SEI formation and better compatibility between the ether-based electrolyte and the hard carbon anode [35].

3.3. Process design and evaluation

Ultimately, the whole process of the proposed sustainable biorefinery was simulated and evaluated for industrial applications. The process integrated biomass pyrolysis, catalytic reforming of pyro-vapors, and two-stage biochar thermal treatment processes based on the experimental results of the best testing cycle. It also integrated gas conditioning, water gas shift (WGS), and vacuum pressure swing adsorption (VPSA) based on data from both literature and industrial experiments (Fig. 1, Fig. S4, S5). Overall, the proposed process yielded 75 kg of H₂ (99.9% purity), 169 kg of HCs, and 891 kg of CO₂ (95% purity) per metric ton of biomass waste (Fig. 7A, Table S15). A total of 2162 kW of power was required to convert each metric ton of biomass waste. It is possible to recover 848 kW of power (141 kW from the catalytic reforming unit, 486 kW from the water gas shift unit, and 221 kW from the electricity offset). All of these values contributed to a net energy consumption of approximately 1314 kW of the process

(Fig. 7B). The catalytic reforming unit was the most energy-intensive among all units in the process, which accounted for approximately 28% (without the energy recovery) and 35% (with the energy recovery) of the total energy requirement (Fig. 7B).

3.4. Techno-economic assessment

The performance of our proposed process with a designed plant capacity of 20 MW_{HHV-biomass} was evaluated by calculating the total capital investment (TCI), the operating expenditures (OPEX), the break-even point (BEP) of HCs, and the payback period (PBP) based on the projected market prices. The calculated TCI of the overall process (20 MW_{HHV-biomass} and 8000 h per year) was approximately €30 million (Figure S13). The total equipment costs of the project were mainly driven by the capital expenditures associated with VPSA system (31.4%), reforming reactors (17.6%) and the pyrolysis unit (8.4%). The other main capital expenditure was the heat recovery and integration systems, including the gas engine unit (20.0%). OPEX constituted a significant portion of the overall system cost throughout the operational lifespan of the plant, with an estimated annual OPEX of around €10.7 million (Figure S14). The main contributors to the OPEX were biomass feedstock (45%), electricity cost (22%) and labor cost (15%).

Based on the outcomes of the experiment, the lifetime of the NiAlO catalyst is a significant unpredictable factor that could greatly affect the overall process. By estimating a catalyst lifetime of 6 months and NiAlO catalyst price of 5 €/kg, the

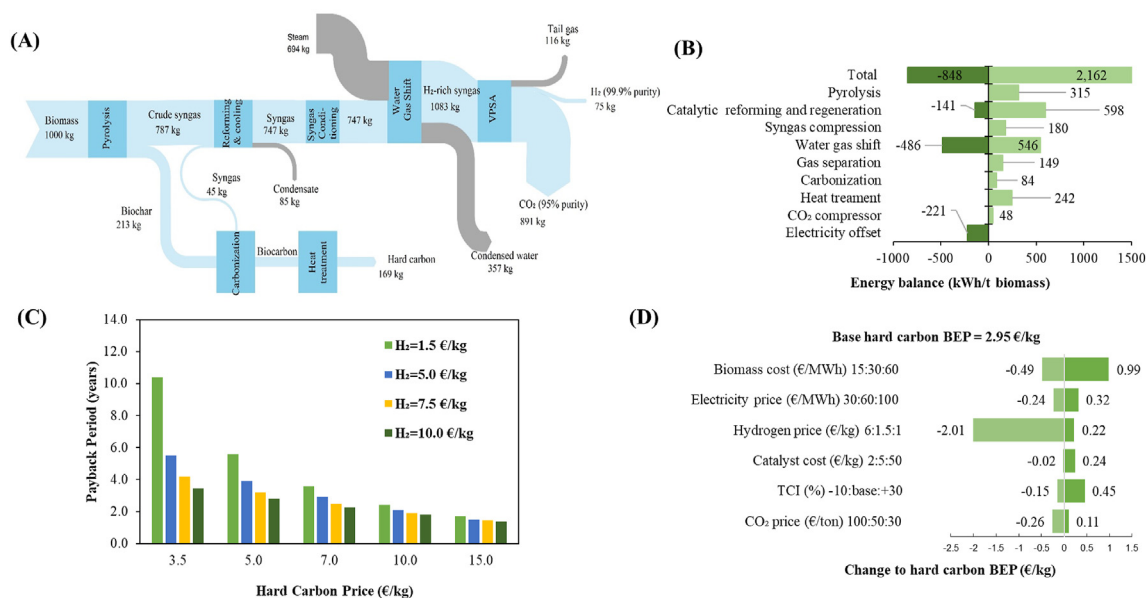


Fig. 7 – Techno-economic analysis (TEA) of the biorefinery process model. A. Mass flow of the process model; B. Energy balance results of the process model; C. Calculated payback period (years) at different H₂ and HC prices; D. Change to HC break-even point caused by parameters variation.

cost associated with catalysts represented a relatively smaller portion of the overall OPEX.

In the BEP calculation for HCs, the H₂ price was assumed as the average production cost of its fossil-based counterparts, commonly referred to as grey H₂, which was estimated at 1.5 €/kg. The catalyst cost has a minimal impact on the break-even point (BEP) for HCs, assuming a lifetime of 6 months. In the analysis, it was assumed that the captured CO₂ would be stored permanently. To account for the value of emissions reductions and incentivize carbon capture, a carbon price of 50 €/ton of captured CO₂ was used, based on the proposal of a support system for BECCS in Sweden [36]. The early stage of bulk production and emerging market application of HCs lead to high retail prices, ranging from 4 €/kg to 3700 €/kg [29]. Based on a reasonable HCs price range of 3.5–15 €/kg, the PBP of the process varied from 2 to 11 years (Fig. 7C). By using the current market price of battery-use synthetic graphite at 13.7 €/kg as a reference, the PBP of the process can be significantly shortened to just 2 years. Furthermore, this study estimated that the BEP of HCs was 2.95 €/kg at an H₂ price of 1.5 €/kg. This suggests that the process can produce affordable HCs that can compete with battery-use graphite, along with renewable H₂ (or green H₂) priced similarly to grey H₂.

Currently, green H₂ produced from water electrolysis costs around 2.5–5.5 €/kg depending on electricity prices [37]. The amount of subsidies for renewable H₂ is still under discussion at national levels. The Dutch government, for instance, has proposed subsidies for H₂ in the range of 3.39–5.83 €/kg [38]. With an H₂ price of 5.0 €/kg and taking into account the proposed government subsidies for green H₂, the BEP of HCs can be significantly reduced to 1.0 €/kg. Considering a green H₂ price of 5.0 €/kg and an HCs price of 13.7 €/kg, the PBP of

the process would not exceed 2 years (Fig. 7C). These findings suggest the excellent profitability of the proposed process.

A single-point sensitivity analysis was also conducted to identify the parameters with the largest influence on the economic feasibility (Fig. 7D) and to estimate the uncertainty in the process model due to a lack of data or price volatility. Given that the feedstock cost represents a significant proportion of the overall product cost, this factor will consistently have a substantial impact on the economic viability of the process. On the other hand, electricity price has a relatively lower impact on the BEP. At a lower electricity price of 30 €/MWh, the BEP would be lowered by around 8%. The selling price of CO₂ as negative emissions moderately affects the overall system profitability. Around a 10% reduction in the BEP of HCs could be expected by an increase in CO₂ price to 100 €/ton. When the NiAlO catalyst lifetime is decreased to as short as one week, which means the amount of catalyst consumed is significantly increased, there is only a 3% increase in the break-even point (BEP) of HCs. On the other hand, if the catalyst lifetime is extended to two years, there is a minimal impact on the BEP of HCs. Therefore, it can be concluded that the catalyst cost has a minimal impact on the economic performance of the overall system.

3.5. Life cycle assessment

The largest driving force for using renewable biomass is its carbon-neutral merit. A life cycle assessment (LCA) of the proposed process was performed in this study. The whole process was designed to be driven by electricity. Electrification of chemical processes can significantly reduce process energy losses, thereby reducing process emissions, and is therefore heavily promoted [39]. The emission parameters of Europe

(EU) electricity mix, Sweden (SE) electricity mix, and SE wind electricity (100% renewable electricity) were considered in the LCA calculation. The LCA results estimated low global warming potentials (GWPs) for our proposed process (0.39 kg CO₂-eq/kg-biomass based on EU electricity mix; 0.11 kg CO₂-eq/kg-biomass based on SE electricity mix; 0.08 kg CO₂-eq/kg-biomass based on SE wind electricity, Fig. 8A). More importantly, the LCA results also showed a negative GWPs value of -0.89 kg CO₂-eq/kg-biomass attributed to the permanent storage of the captured CO₂ (Fig. 8A).

The GWPs for H₂ production of the proposed process were 5.21 kg CO₂-eq/kg-H₂, 1.45 kg CO₂-eq/kg-H₂, and 1.02 kg CO₂-eq/kg-H₂ based on EU electricity mix, SE electricity mix, and SE wind electricity (Fig. 8B), respectively. When using 100% renewable electricity, i.e., SE wind electricity, the proposed process can reduce the emissions by 89% compared to the fossil-based counterpart (9 kg CO₂-eq/kg-H₂ from SMR (14), Fig. 8B). If the H₂ production from the fossil-based process includes CO₂ capture and storage (CCS, 3.5 kg CO₂-eq/kg-H₂ from SMR with CO₂ capture, [40]), the process would also reduce emissions by 72% (Fig. 8B). The proposed process can also reduce the emissions by 62%, compared to a conventional biomass gasification process (2.68 kg CO₂-eq/kg-H₂, Fig. 8B). All these results indicated a low-carbon footprint in H₂ production. Taking CO₂ capture into consideration, the net GWPs for H₂ production of the proposed process were calculated to be -10.85 kg CO₂-eq/kg-H₂ when using SE wind electricity (Fig. 8B). The GWPs for HCs production of the proposed

process were 2.34 kg CO₂-eq/kg-HCs, 0.64 kg CO₂-eq/kg-HCs, and 0.45 kg CO₂-eq/kg-HCs based on EU electricity mix, SE electricity mix, and SE wind electricity (Fig. 8C). When using 100% renewable electricity, the proposed process can reduce the emissions by approximately 92% and 97% compared to the fossil-based counterparts of natural graphite (5.82 kg CO₂-eq/kg-graphite, Ecoinvent.2021) and synthetic graphite (13.8 kg CO₂-eq/kg-graphite, Ecoinvent.2021), respectively (Fig. 8C). Compared to the process of bio-HCs production reported in the literature (5.66 kg CO₂-eq/kg-HCs, [41]), the proposed process can also reduce emissions by 92% (Fig. 8C). Considering the captured CO₂, the net GWPs for HCs production of the proposed process was -4.78 kg CO₂-eq/kg-HCs when using SE wind electricity (Fig. 8C). Notably, a conservative approach was taken where all burdens are allocated to only one of the evaluated products. Once a co-product allocation is implemented, the GWPs for H₂ and HCs productions of the proposed process could be even lower. The proposed process is expected to produce low-carbon footprint end products while achieving substantial negative emissions. To determine the impact of the catalyst lifetime on the emission value of the product, we conducted a sensitivity analysis. The catalyst-associated emission has a minimal impact on the overall process emission, assuming a lifetime of 6 months. Despite the NiAlO catalyst having a lifetime as short as one week, the proposed process for HCs and H₂ production shows negligible changes in net GWPs (Fig. 8D). This suggests that the catalyst has a negligible impact on the emission of the process.

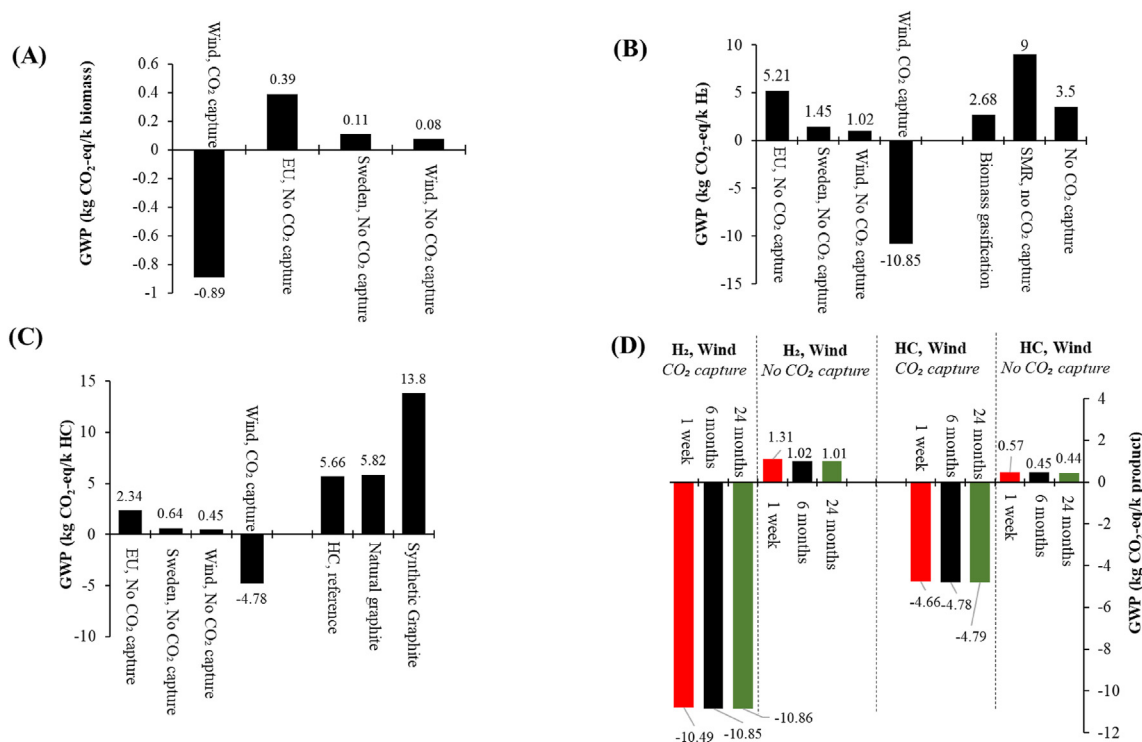


Fig. 8 – Life cycle assessment (LCA) of the biorefinery process model. **A.** Calculated global warming potential results on the basis of the process; **B.** Calculated global warming potential results on the basis of the hydrogen production; **C.** Calculated global warming potential results on the basis of the hard carbon production; **D.** Influence of the NiAlO catalyst lifetime on the calculated global warming potential for hydrogen and hard carbon.

4. Conclusions

A sustainable and feasible biorefinery was proposed to achieve the carbon-negative utilization of biomass waste into affordable green hydrogen and battery anodes. The main conclusions are shown below:

- A tandem biocarbon + NiAlO spinel + biocarbon reforming catalyst was constructed, wherein biomass pyrolysis vapors were efficiently and stably converted into H₂+CO (as a mixture) through the selective promotion of different types of reactions in different catalyst layers. The proposed catalyst strategy yielded over 91 wt% of syngas with H₂+CO proportion over 83 vol%.
- A two-step thermal treatment process was integrated to convert the biomass pyrolysis residues into high-quality hard carbons as sodium ion battery anodes. Full cell assembly by using the HC-1600-6h sample as anode showed superior performance (263 Wh/kg with ICE of 89%). Characterization results showed that the HC-1600-6h structure rich in nano graphitic domains and closed pores demonstrated superior electrochemical performance.
- The overall process was designed, simulated and evaluated based on the above processes. The simulation results showed that 75 kg of H₂ (99.9% purity), 169 kg of HCs, and 891 kg of CO₂ (95% purity) could be produced per metric ton of biomass waste. The life cycle assessment estimated a negative-emission biomass waste valorization process (−0.81 CO₂-eq/kg-biomass based on Sweden wind electricity). Without consideration of the negative emission, the process could also produce a low-carbon footprint of H₂ (1.01 kg CO₂-eq/kg-H₂, based on Sweden wind electricity) and hard carbon (0.44 kg CO₂-eq/kg-HCs, based on Sweden wind electricity). The techno-economic assessment predicted a highly profitable process that produces cost-effective H₂ and hard carbon battery anodes. The payback period of the process will not exceed two years at reference prices of 13.7 €/kg and 5 €/kg for HCs and H₂. The cost of the catalyst and its associated emissions have minimal impact on the economic performance and overall emissions of the process.

Declaration of competing interest

None.

Acknowledgements

Financial supported by VINNOVA- the Swedish innovation fund Agency with project number 2021-03735 is highly appreciated. One of the authors, Hanmin Yang would like to acknowledge the financial support from the Chinese Scholarship Council (CSC) and Stiftelsen Energitekniskt Centrum i Piteå, Sweden.

Appendix A. Supplementary data

Supplementary data to this article can be found online at <https://doi.org/10.1016/j.ijhydene.2023.09.096>.

REFERENCES

- [1] Jacobson MZ. Review of solutions to global warming, air pollution, and energy security. *Energy Environ Sci* 2009;2:148–73.
- [2] Nguyen VG, Nguyen-Thi TX, Phong Nguyen PQ, Tran VD, Agbulut Ü, Nguyen LH, et al. Recent advances in hydrogen production from biomass waste with a focus on pyrolysis and gasification. *Int J Hydrogen Energy* 2023. In press.
- [3] Tilman D, Socolow R, Foley JA, Hill J, Larson E, Lynd L, Pacala S, Reilly J, Searchinger T, Somerville C. Beneficial biofuels—the food, energy, and environment trilemma. *Science* 2009;325:270–1.
- [4] Hassan Q, Abdulateef AM, Hafedh SA, Al-samari A, Abdulateef J, Sameen AZ, Salman HM, Al-Jiboory AK, Wieteska S, Jaszczur M. Renewable energy-to-green hydrogen: a review of main resources routes, processes and evaluation. *Int J Hydrogen Energy* 2023;48:17383–408.
- [5] Anderson K, Peters G. The trouble with negative emissions. *Science* 2016;354:182–3.
- [6] Bellamy R. Incentivize negative emissions responsibly. *Nat Energy* 2018;3:532–4.
- [7] Ubando AT, Felix CB, Chen W-H. Biorefineries in circular bioeconomy: a comprehensive review. *Bioresour Technol* 2020;299:122585.
- [8] Tao L, Schell D, Davis R, Tan E, Elander R, Bratis A. NREL 2012 achievement of ethanol cost targets: biochemical ethanol fermentation via dilute-acid pretreatment and enzymatic hydrolysis of corn stover. Golden, CO (United States): National Renewable Energy Lab.(NREL); 2014.
- [9] Rodionova MV, Bozieva AM, Zharmukhamedov SK, Leong YK, Chi-Wei Lan J, Veziroglu A, Veziroglu TN, Tomo T, Chang J-S, Allakhverdiev SI. A comprehensive review on lignocellulosic biomass biorefinery for sustainable biofuel production. *Int J Hydrogen Energy* 2022;47:1481–98.
- [10] Awasthi MK, Sindhu R, Sirohi R, Kumar V, Ahluwalia V, Binod P, Juneja A, Kumar D, Yan B, Sarsaiya S, Zhang Z, Pandey A, Taherzadeh MJ. Agricultural waste biorefinery development towards circular bioeconomy. *Renew Sustain Energy Rev* 2022;158:112122.
- [11] Liao Y, Koelewijn S-F, Van Den Bossche G, Van Aelst J, Van Den Bosch S, Renders T, Navare K, Nicolai T, Van Aelst K, Maesen M, Matsushima H, Thevelein JM, Van Acker K, Lagrain B, Verboekend D, Sels BF. A sustainable wood biorefinery for low-carbon footprint chemicals production. *Science* 2020;367:1385–90.
- [12] Usmani Z, Sharma M, Awasthi AK, Lukk T, Tuohy MG, Gong L, Nguyen-Tri P, Goddard AD, Bill RM, Nayak SC. Lignocellulosic biorefineries: the current state of challenges and strategies for efficient commercialization. *Renew Sustain Energy Rev* 2021;148:111258.
- [13] Sridevi V, Surya DV, Reddy BR, Shah M, Gautam R, Kumar TH, et al. Challenges and opportunities in the production of sustainable hydrogen from lignocellulosic biomass using microwave-assisted pyrolysis: a review. *Int J Hydrogen Energy* 2023. In press.

- [14] Wachsmuth J, Aydemir A, Döscher H, Eckstein J, Poganietz W-R, François DE, Scheer D. The potential of hydrogen for decarbonizing EU industry. 2021.
- [15] Xie L, Tang C, Bi Z, Song M, Fan Y, Yan C, Li X, Su F, Zhang Q, Chen C. Hard carbon anodes for next-generation Li-ion batteries: review and perspective. *Adv Energy Mater* 2021;11:2101650.
- [16] Escobar B, Martínez-Casillas DC, Pérez-Salcedo KY, Rosas D, Morales L, Liao SJ, Huang LL, Shi X. Research progress on biomass-derived carbon electrode materials for electrochemical energy storage and conversion technologies. *Int J Hydrogen Energy* 2021;46:26053–73.
- [17] Strefler J, Kriegler E, Bauer N, Luderer G, Pietzcker RC, Giannousakis A, Edenhofer O. Alternative carbon price trajectories can avoid excessive carbon removal. *Nat Commun* 2021;12:2264.
- [18] Lights N. Accelerating decarbonisation. 2021.
- [19] Wang Y, Sun G, Dai J, Chen G, Morgenstern J, Wang Y, Kang S, Zhu M, Das S, Cui L, Hu L. A high-performance, low-tortuosity wood-carbon monolith reactor. *Adv Mater* 2017;29:1604257.
- [20] Sun P, Elgowainy A. Updates of hydrogen production from SMR process in GREET® 2019. Lemont, IL, USA: Argonne National Laboratory; 2019.
- [21] Mettler MS, Vlachos DG, Dauenhauer PJ. Top ten fundamental challenges of biomass pyrolysis for biofuels. *Energy Environ Sci* 2012;5.
- [22] Ren J, Cao J-P, Zhao X-Y, Liu Y-L. Recent progress and perspectives of catalyst design and downstream integration in biomass tar reforming. *Chem Eng J* 2022;429:132316.
- [23] Arregi A, Barbarias I, Alvarez J, Erkiaga A, Artetxe M, Amutio M, Olazar M. Hydrogen production from biomass pyrolysis and in-line catalytic steam reforming. *Chemical Engineering Transactions* 2015;43:547–52.
- [24] Yang H, Cui Y, Han T, Sandström L, Jönsson P, Yang W. High-purity syngas production by cascaded catalytic reforming of biomass pyrolysis vapors. *Appl Energy* 2022;322:119501.
- [25] Remiro A, Arandia A, Oar-Arteta L, Bilbao J, Gayubo AG. Regeneration of NiAl₂O₄ spinel type catalysts used in the reforming of raw bio-oil. *Appl Catal B Environ* 2018;237:353–65.
- [26] Benrabaa R, Barama A, Boukhlof H, Guerrero-Caballero J, Rubbens A, Bordes-Richard E, Löfberg A, Vannier R-N. Physico-chemical properties and syngas production via dry reforming of methane over NiAl₂O₄ catalyst. *Int J Hydrogen Energy* 2017;42:12989–96.
- [27] Buentello-Montoya D, Zhang X, Li J, Ranade V, Marques S, Geron M. Performance of biochar as a catalyst for tar steam reforming: effect of the porous structure. *Appl Energy* 2020;259:114176.
- [28] Shen Y, Fu Y. Advances in in situ and ex situ tar reforming with biochar catalysts for clean energy production. *Sustain Energy Fuels* 2018;2:326–44.
- [29] Liu H, Baumann M, Dou X, Klemens J, Schneider L, Wurba A-K, Häringer M, Scharfer P, Ehrenberg H, Schabel W. Tracing the technology development and trends of hard carbon anode materials-A market and patent analysis. *J Energy Storage* 2022;56:105964.
- [30] Zhao C, Wang Q, Lu Y, Li B, Chen L, Hu Y-S. High-temperature treatment induced carbon anode with ultrahigh Na storage capacity at low-voltage plateau. *Sci Bull* 2018;63:1125–9.
- [31] Dou X, Hasa I, Saurel D, Vaalma C, Wu L, Buchholz D, Bresser D, Komaba S, Passerini S. Hard carbons for sodium-ion batteries: structure, analysis, sustainability, and electrochemistry. *Mater Today* 2019;23:87–104.
- [32] Chayambuka K, Mulder G, Danilov DL, Notten PH. From li-ion batteries toward Na-ion chemistries: challenges and opportunities. *Adv Energy Mater* 2020;10:2001310.
- [33] Fichtner M. Recent research and progress in batteries for electric vehicles. *Batteries & Supercaps* 2022;5:e202100224.
- [34] Meng Q, Lu Y, Ding F, Zhang Q, Chen L, Hu Y-S. Tuning the closed pore structure of hard carbons with the highest Na storage capacity. *ACS Energy Lett* 2019;4:2608–12.
- [35] Bhawana K, Roy A, Chakrabarty N, Gautam M, Dutta DP, Mitra S. Sodium-ion batteries: chemistry of biomass derived disordered carbon in carbonate and ether-based electrolytes. *Electrochim Acta* 2022;425:140744.
- [36] S.E. Agency. Förslag på utformning av ett stödsystem för bio-CCS". 2021.
- [37] E. Commission. Questions and answers: a hydrogen strategy for a climate neutral Europe. 2020.
- [38] Buiteveld J. Techno-economic evaluation of a novel biomass pyrogasification process with an integrated sorption-shift system: a process for the conversion of waste to high-quality biochar and hydrogen with carbon capture and hydrogen upgrading. University of Twente; 2021.
- [39] Wismann ST, Engbæk JS, Vendelbo SB, Bendixen FB, Eriksen WL, Aasberg-Petersen K, Frandsen C, Chorkendorff I, Mortensen PM. Electrified methane reforming: a compact approach to greener industrial hydrogen production. *Science* 2019;364:756–9.
- [40] Trippe F, Fröhling M, Schultmann F, Stahl R, Henrich E. Techno-economic assessment of gasification as a process step within biomass-to-liquid (BtL) fuel and chemicals production. *Fuel Process Technol* 2011;92:2169–84.
- [41] Xu Z, Wang J, Guo Z, Xie F, Liu H, Yadegari H, Tebyetekerwa M, Ryan MP, Hu YS, Titirici MM. The role of hydrothermal carbonization in sustainable sodium-ion battery anodes. *Adv Energy Mater* 2022;12:2200208.